Supporting Information

Depressing Relaxation and Conduction Loss of Polar Polymer Materials by Inserting Bulky Charge Traps for Superior Energy Storage Performance in High-pulse Energy Storage Capacitors Application

Meirong Zhang[a], Bofeng Zhu[b], Xiao Zhang[b], Zhenxue Liu[c], Xiaoyong Wei[d]*, Zhicheng Zhang[a]**

a Department of Applied Chemistry, Xi'an Key Laboratory of Sustainable Energy Materials Chemistry, School of Chemistry, Xi'an Jiaotong University, Xi'an 710049, P. R. China

b National Key Laboratory of Science and Technology on Vessel Integrated Power System, Naval University of Engineering, Wuhan 430034, P. R. China

cShandong Chambroad Holding Group Co., Ltd., Binzhou, Shandong Province, 256500, P. R. China.

d Electronic Materials Research Laboratory, Key Laboratory of the Ministry of Education and International Center for Dielectric Research, School of Electronic and Information Engineering, Xi'an Jiaotong University, Xi'an 710049, P. R. China

[*]Corresponding Authors. E-mail: zhenxue.liu@chambroad.com

[**]Corresponding Authors. E-mail: wdy@mail.xjtu.edu.cn; (X.Y. Wei)

[***]Corresponding Authors. E-mail: zhichengzhang@mail.xjtu.edu.cn; (Z.C. Zhang)

Characterization

^{1}H NMR spectra (JEOL JNM-ECZ400S/L1, 400 MHz, JEOL, Japan) were used to detect and characterize the composition and structure of the P(MMA-VQQ). The ultraviolet absorption spectra of fabricated polymer and films were measured by ultraviolet-visible near-infrared spectrophotometer (PE Lambda950, United States). The number-average molecular weight (M_n) and Polymer dispersity index (PDI) of P(MMA-VQQ) were characterized by Gel Permeation Chromatography (WATERS ACQUITY APC, MALVERN OMNISEC REVEAL, United States). The glass transition temperatures (T_g) were characterized by differential scanning calorimetry (DSC) (Netzsch, 214 Polymer DSC21400A-0466-L, Germany) with a heating rate of 10^{o}C min^{-1}. The thermostability of the fabricated films was conducted on a thermogravimetric analysis (TGA 2 (LF), Mettler-Toledo, Swiss) under a nitrogen atmosphere and accompanied with a heating rate of 10^{o}C min^{-1} (30 ~ 800^{o}C). The both side gold electrodes of films were sputtered by ionized sputtering apparatus (JEOL, JFC1600 autofine coater, Japan). The dielectric performance and thermally stimulated depolarization currents (TSDC) of the films were carried on broadband dielectric spectrometer (BDS) (Novocontrol, Concept 80, Germany). Displacement-electric (*D-E*) loops, leakage current density and charge-discharge cycling stability were measured on ferroelectric tester (Radiant Technologies, Premiere II, United States). The breakdown strength of fabricated film was evaluated by High-voltage direct current power supply (RK2674B, China). In the rapid charge-discharge experiments, films were charged to a given voltage using a high voltage MOSFET switch (610D-K-CE-IX); the inner resistance (RL) was 100 kΩ, and the discharge curve was measured under varied temperatures. Density functional theory (DFT) simulation reveals the changes of distribution of electrostatic potential and molecular orbital energy levels of molecular models. Specifically, DFT calculation was conducted by B3LYP hybrid function and the 3-21 G basis function in Gaussian 09.

The synthesis of 3-Vinyl-quinoline:

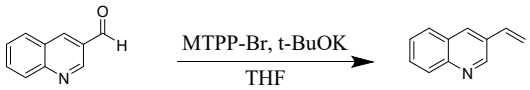

Scheme S1 Synthesis approach of 3-Vinyl-quinoline through Wittig reaction.

A mixture of 3-quinolinecarboxaldehyde (1 g, 6.36 mmol) and methyltriphenylphosphonium bromide (2.5 g, 6.97 mmol) in dry THF (40 mL) was stirred at 0°C for 30 min under N_2 atmosphere. Then, *t*-BuOK (0.78 g, 6.97 mmol) was added in portions and the reaction was stirred at room temperature for 24 h. After this time, 50 mL of water was added and the organic layer extracted twice with CH_2Cl_2. The combined organic layers were washed twice with water, dried over anhydrous Na_2SO_4 and the solvent evaporated under vacuum. The resulting crude product was purified using a neutral alumina chromatographic column using hexane as eluent to obtain a yellow oil in 75% yield. ^{1}H NMR ($CDCl_3$, 400 MHz): δ (ppm) 8.06 (dd, 1H, J = 9.08 Hz, Ar-H), 8.03 (dd, 1H, J = 8.80 Hz, Ar-H), 7.71 (d, 1H, J = 7.98 Hz, Ar-H), 7.65 (t, 1H, J = 6.80 Hz, Ar-H), 7.54 (d, 1H, J = 8.53 Hz, Ar-H), 7.44 (t, 1H, J = 7.153 Hz, Ar-H), 7.00 (q, 1H, =C–H), 6.23 (d, 1H, J = 17.61 Hz, =C–H), 5.62 (d, 1H, J = 10.73 Hz, =C–H).

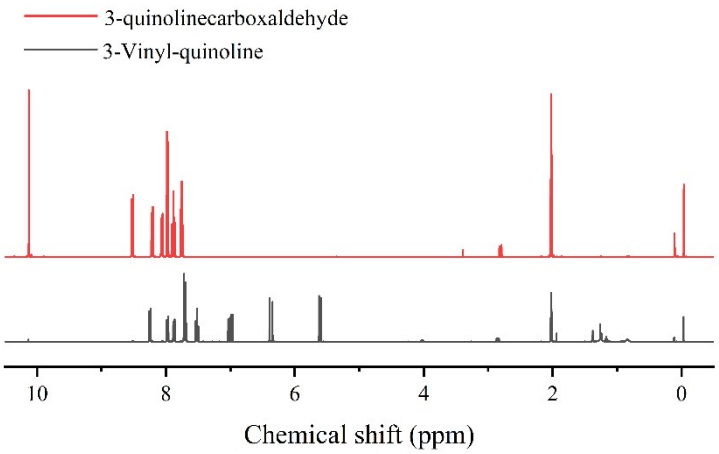

Figure S1. ^{1}H NMR spectra of 3-quinolinecarboxaldehyde and 3-Vinyl-quinoline.

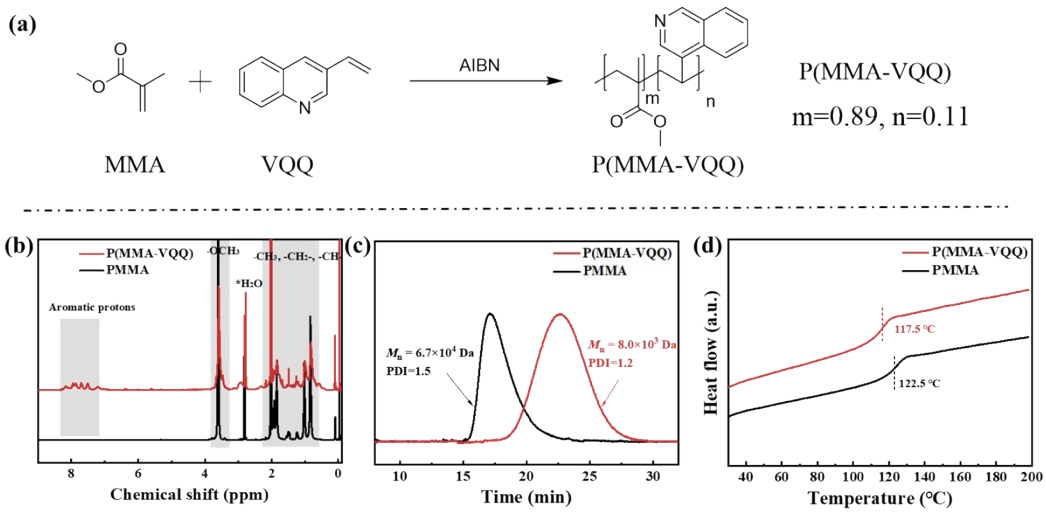

Figure S2. (a) Synthesis approach of P(MMA-VQQ) by bulk polymerization; (b) ^{1}H NMR spectra of PMMA and P(MMA-VQQ); (c) GPC curve of PMMA and P(MMA-VQQ); (d) DSC thermograms of PMMA and P(MMA-VQQ).

Figure S2a shows the procedure for synthesizing the traces content of electron-deficient quinoline incorporated random copolymers P(MMA-VQQ). The composition proportion of P(MMA-VQQ) could be precise characterized by ^{1}H NMR as presented in Figure S2b. The resonance signal at 8.2-7.0 ppm is assigned to quinoline ring protons, and the proton peak at 3.8 to 3.6 ppm is referring to the methoxy of PMMA. The proton signals from 2.5 to 0.5 ppm are attributed to the methyl, methylene and methine of PMMA. Therefore, the molar proportion of quinoline units in the P(MMA-VQQ) was 11 mol%, which was calculated using following equation (S1). Subsequently, the GPC curve was obtained to analyze the macular weight and polymer dispersity index of fabricated polymer. As shown in Figure S2c, the number-average molecular weight (M_n) of homopolymer PMMA was much higher than copolymer P(MMA-VQQ), which was resulting from that electron-deficient quinoline group weaken the polymerization activity of vinyl. DSC results in Figure S2d illustrated that extremely low content of quinoline scarcely changed the thermal stability of PMMA.

$$\mathrm{mol}/\%_{(\mathrm{VQQ})} = \frac{3\int_{7.0}^{8.2} CH_{(\mathrm{VQQ})}}{8\int_{3.6}^{3.8} CH_{(\mathrm{MMA})} + 3\int_{7.0}^{8.2} CH_{(\mathrm{VQQ})}} \qquad \text{(S1)}$$

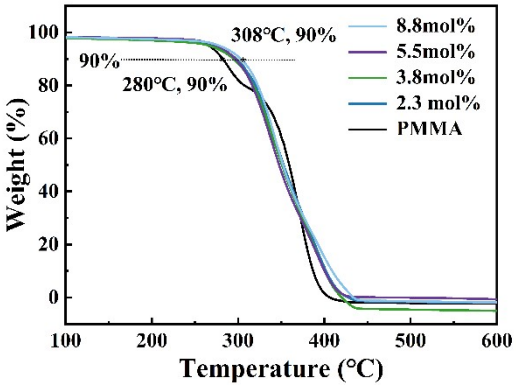

Figure S3. Thermal decomposition of fabricated films.

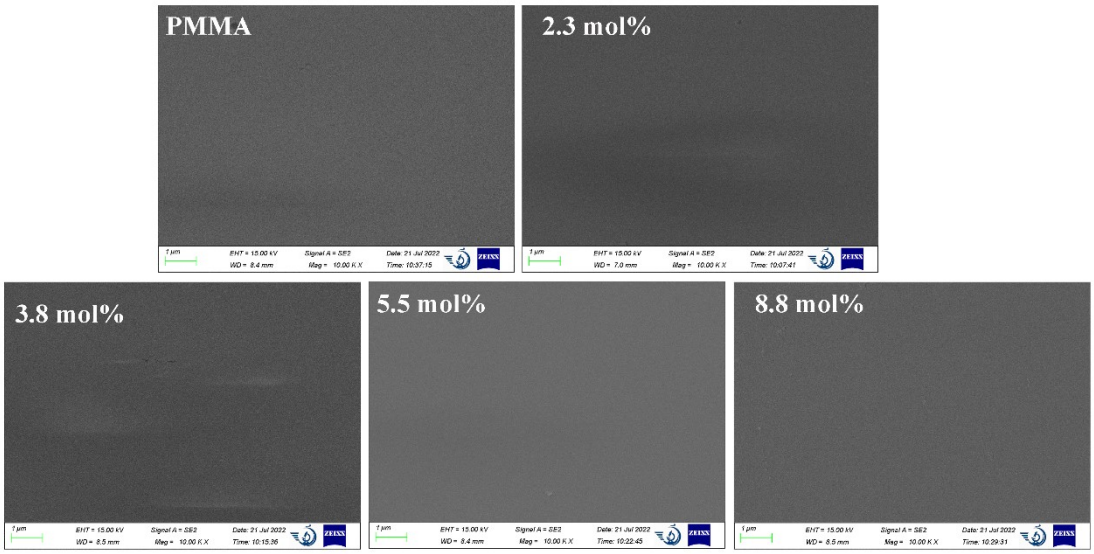

Figure S4. Surface SEM images of fabricated polymers.

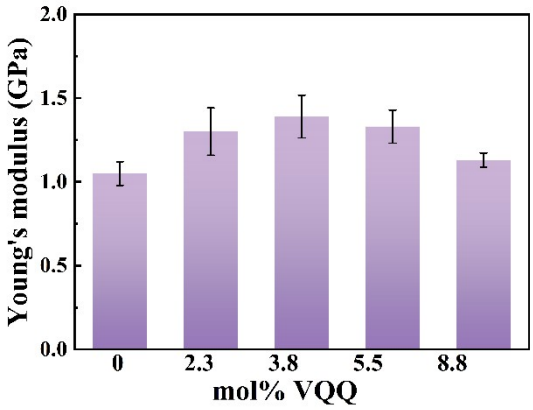

Figure S5. Young's modules for fabricated film.

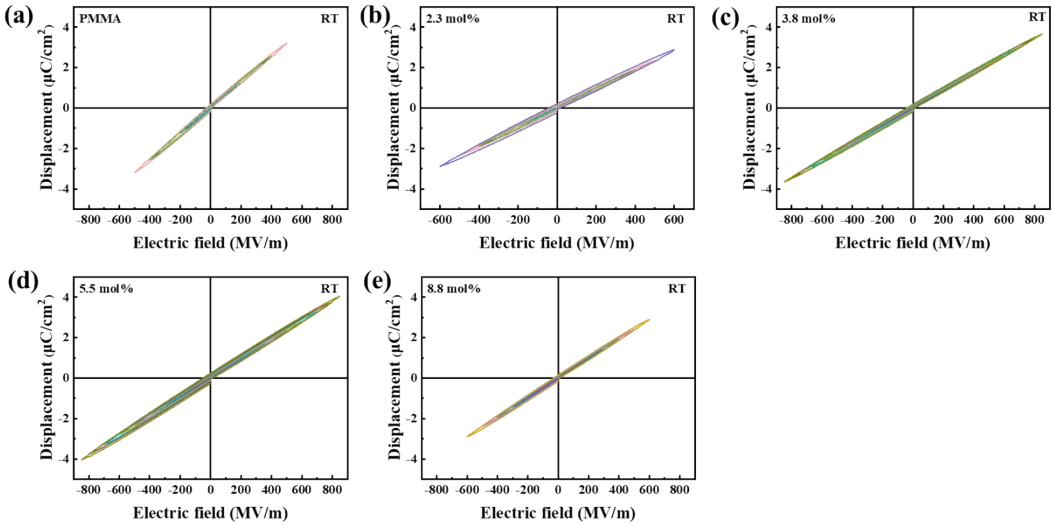

Figure S6. Bipolar *D-E* loops for fabricated materilas at room temperature.

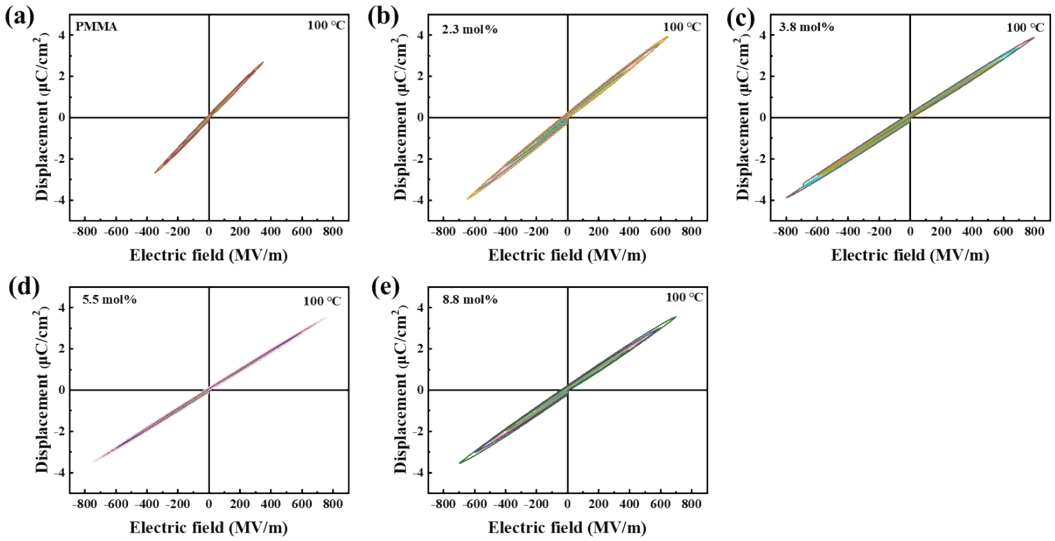

Figure S7. Bipolar *D-E* loops for fabricated materilas 100ºC.

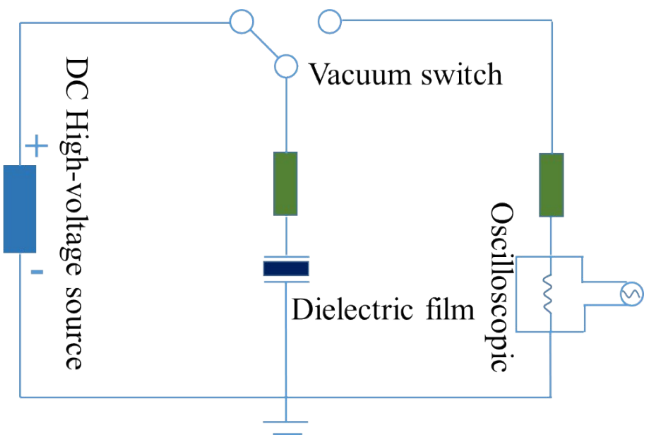

Figure S8. Schematic circuit of the discharge experiment.

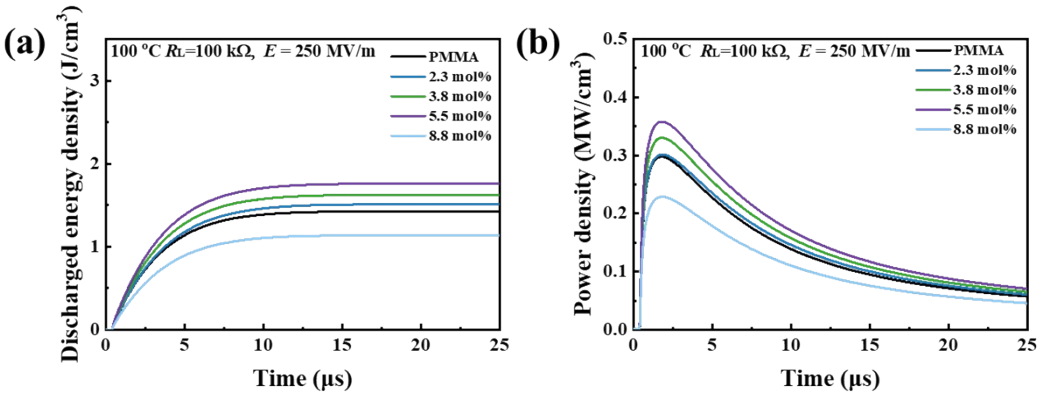

Figure S9. (a) and (b) discharged energy density and power density of fabricated polymers at at 100°C.

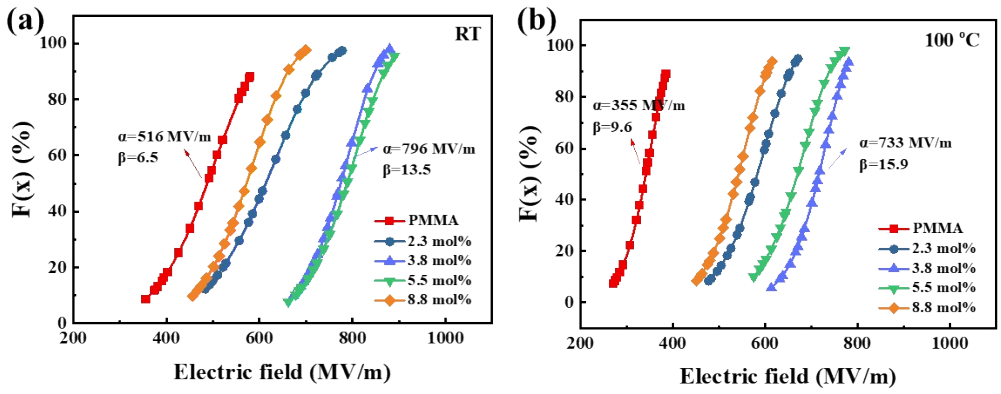

Figure S10. (a) and (b) Weibull distribution of the measured breakdown fields for all polymers at ambient temperature and 100°C.